



**Fermi National Accelerator Laboratory**

**FERMILAB-Conf-99/090**

## **Fixed Field Circular Accelerator Designs**

C. Johnstone and W. Wan

*Fermi National Accelerator Laboratory  
P.O. Box 500, Batavia, Illinois 60510*

A. Garren

*UCLA  
Los Angeles, California 90024*

January 2000

Published Proceedings of the *Particle Accelerator Conference, PAC 99*,  
New York, New York, March 29-April 2, 1999

## **Disclaimer**

*This report was prepared as an account of work sponsored by an agency of the United States Government. Neither the United States Government nor any agency thereof, nor any of their employees, makes any warranty, expressed or implied, or assumes any legal liability or responsibility for the accuracy, completeness, or usefulness of any information, apparatus, product, or process disclosed, or represents that its use would not infringe privately owned rights. Reference herein to any specific commercial product, process, or service by trade name, trademark, manufacturer, or otherwise, does not necessarily constitute or imply its endorsement, recommendation, or favoring by the United States Government or any agency thereof. The views and opinions of authors expressed herein do not necessarily state or reflect those of the United States Government or any agency thereof.*

## **Distribution**

*Approved for public release; further dissemination unlimited.*

## **Copyright Notification**

*This manuscript has been authored by Universities Research Association, Inc. under contract No. DE-AC02-76CH03000 with the U.S. Department of Energy. The United States Government and the publisher, by accepting the article for publication, acknowledges that the United States Government retains a nonexclusive, paid-up, irrevocable, worldwide license to publish or reproduce the published form of this manuscript, or allow others to do so, for United States Government Purposes.*

# Fixed Field Circular Accelerator Designs \*

**C. Johnstone**,<sup>†</sup> and **W. Wan**, FNAL, Batavia, IL 60510  
**A. Garren**, UCLA, Los Angeles, CA 90024

## Abstract

The rapid rate and cycle time required to efficiently accelerate muons precludes conventional circular accelerators. Recirculating linacs provide one option, but the separate return arcs per acceleration pass may prove costly. Recent work on muon acceleration schemes has concentrated on designing fixed-field circular accelerators whose strong superconducting fields can sustain a factor of 4 increase in energy from injection to extraction. A 4 to 16 GeV fixed-field circular accelerator has been designed which allows large orbit excursions and the tune to vary as a function of momentum. Acceleration is .6 GeV per turn so the entire cycle consists of only 20 turns. In addition a 16 to 64 GeV fixed-field circular accelerator has been designed which is more in keeping with the traditional Fixed Field Alternating Gradient machines[2]. In this work the two machine designs are described.

## 1 INTRODUCTION

Rapid acceleration in a multi-stage system is needed for a muon collider to limit intensity loss from muon decay. For the lower-energy acceleration stages, this consideration dominates the design. Ultra-rapid cycling synchrotrons and recirculating linacs with multiple return arcs have been considered for muon accelerators[1]. Given the technical complexity or expense of these proposed schemes, the idea of using fixed-field, single-path accelerators has been revisited in recent work. The arcs of such machines, composed of large-aperture, single-bore superconducting magnets, can be designed to accomodate the large energy range from acceleration. Lattices have been developed which can contain an energy change of a factor of four from injection to extraction. The multistage acceleration scheme considered here employs a linac as the first stage followed by two fixed-field machines, one accelerating from 4 GeV to 16 GeV and the next from 16 GeV to 64 GeV.

The 4-16 GeV stage is a FODO-based cell structure with the goal to maximize bend per cell and minimize overall circumference and intensity loss from decay. The 16-64 GeV stage is similar to an FFAG design developed at MURA[2] whose magnets have a magnetic field characterized by constant radial field indices. The lower energy lattice was optimized for minimum circumference, in consideration of muon lifetime. The higher energy lattice design minimizes aperture (cost), which may be the more important consideration for that energy range. The design approaches varied accordingly. The following sections will describe the two

lattice designs and venture a few comparisons and conclusions.

## 2 FIXED-FIELD LATTICE DESIGN

A circular accelerator system can be designed using magnets with alternating gradient focusing, but with fields that remain constant for the duration of the acceleration cycle. The closed orbits move during the cycle but remain within the (single) aperture of each magnet. Such FFAG rings were first designed and studied at MURA[2], and are distinct from other possible accelerators, such as linacs, pulsed synchrotrons, or recirculating linacs with multiple-path return arcs. The following examples made are intended for use in a low-energy muon collider in a center-of-mass range of about 100 GeV (called a Higgs factory), but the ideas are applicable to higher energy colliders as well.

We will discuss two specific FFAG accelerator designs for the Higgs factory, one accelerates muons from 4 GeV to 16 GeV, the other from 16 GeV to 64 GeV. The rf systems are assumed to deliver on the order of 0.5-2 GeV per turn. In order to explore different possibilities, these two rings use different design approaches, though both are FFAG in the sense mentioned above. The lower and higher energy rings use non-scaling and scaling FFAG lattices respectively. In a non-scaling lattice the orbit properties of the closed orbits are a function of energy, while in a scaling lattice they are independent of energy.

The cells of the low energy, non-scaling ring contain a horizontally focusing quadrupole and a vertically focusing combined-function bending magnet. This magnet configuration was chosen to maximize the net bend per cell for a given magnet aperture, implying the fewest arc cells and minimal ring circumference.

The cells of the high energy, scaling ring contain one F magnet, one D magnet and short drift spaces. Each of the magnets has a magnetic field profile  $B(\rho) \sim \rho^n$ , where  $n$  is negative and positive in the F and D magnets respectively, which gives the AG focusing. In order to decrease the radial aperture, the magnetic field directions also alternate, causing the orbits to curve successively towards and away from the ring center in the F and D magnets, and the closed orbits to describe a scalloped set of parallel curves. To close the ring, the F magnets are made longer than the D magnets.

The non-scaling aproach yields the smallest design circumference, but a radial aperture which is generally larger than in the scaling approach. In the scaling aproach, lattice parameters do not vary with energy and radial excursions and magnet apertures can be reduced, but at the price of a larger circumference.

\* Work supported by the U.S. Department of Energy under contract No. DE-AC02-76HO3000

<sup>†</sup> email: cjj@fnal.gov

### 3 NONSCALING FFAG LATTICE

A nonscaling FFAG lattice relies on a strong-focussing FODO cell composed of large-bore superconducting magnets to contain the large range in momenta. The cell presented here consists of a horizontally-focussing (F) quadrupole followed by a vertically-focussing, combined-function (D) magnet. The cell could also be comprised of separated-function magnets, but the magnetic field layout chosen here produces the largest bend per cell for a given maximum excursion of the closed-orbit during acceleration. (The peak of the closed orbit excursion always occurs at the center of the F quadrupole.)

The optimal lengths of the magnets can be analytically obtained assuming thin lens kicks and imposing closure on both the orbit and lattice functions over a half cell. To solve the equations, the maximum off-axis orbit excursion in the F quadrupole must be chosen along with the F quadrupole's aperture and poletip field. To insure stability in both planes, the D quadrupole strength is taken to be equal to the F quadrupole strength. In the work presented here a maximum closed-orbit excursion of 7 cm has been chosen for the F quadrupole (implying a physical half-aperture of about 10-13 cm horizontally), and a gradient of 70 T-m. The spacing between magnets is taken to be 0.25 m. The aperture required in the combined function magnet will be close to half that of the F quadrupole. In practice, the bend and corresponding length of the combined function magnet must be rescaled to the desired maximum off-axis excursion due to the approximations inherent in the thin lens kick model, keeping the vertical focussing strength of the combined function magnet equal to the F quadrupole strength during the rescaling.

The lattice components and functions of the resulting cell are plotted in Figure 1. Orbit excursions at 4 GeV are plotted in Figure 2. The corresponding orbit excursion at 16 GeV is almost an inversion of the curve in Figure 2. Tunes per cell vary from  $\mu_{x,y} \sim 0.4$  at 4 GeV to  $\mu_{x,y} \sim 0.075$  at 16 GeV. The arc contains about 100 cells, 1.6 m long, giving a total length of 160 m. If one assumes 100 m for rf, then the total circumference of this ring is less than 300 m. Adding an additional 100 m of rf and keeping the same choice of parameters, but scaling the ring to 16 to 64 GeV energy range, increases the circumference to 772 m. The circumference can be compared to the 1.36 km circumference of the 16 to 64 GeV scaling FFAG lattice described below.

The main drawback to this approach is the large pathlength changes as a function of energy. The pathlength shape is parabolic and changes by 70 cm from a minimum at 10 GeV to injection at 4 GeV and extraction at 16 GeV. We are presently studying the needed rf frequency and phasing requirements for different applications to see what is feasible. In subsequent calculations, a fixed-field sextupole component was added to the quadrupole fields to change the parabolic shape of the pathlength variation to one which increases almost monotonically with energy. Chicanes could be incorporated into this version of the lattice to eliminate

pathlength changes at the expense of circumference.

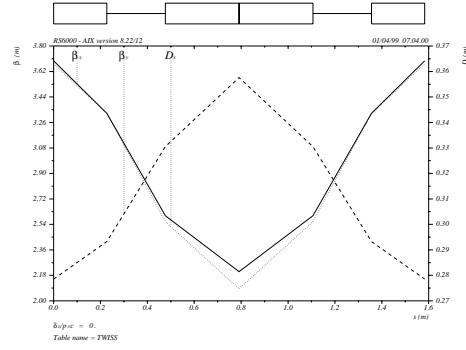


Figure 1: Lattice functions of nonscaling FFAG cell.

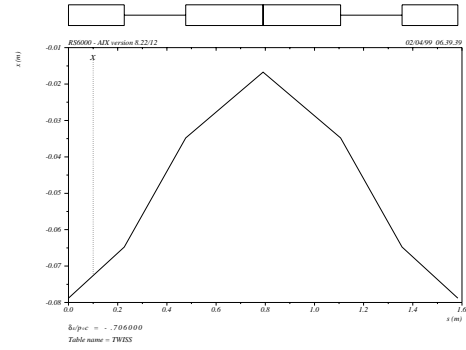


Figure 2: 4 GeV orbit excursion of nonscaling FFAG cell

### 4 SCALING FFAG ACCELERATOR LATTICE

This design is based on FFAG concepts developed at MURA in the 1950s. All of the orbits accelerated traverse a single vacuum tube in one set of magnets, and the radial extent of these orbits is small compared to the radius of the ring.

A cell of this lattice contains one F magnet, one D magnet and short drift spaces. Each of the magnets has a magnetic field  $B(\rho) \sim \rho^n$ , where  $\rho$  is the distance from the local center of curvature of each magnet to the orbit. Hence the field index  $n = -(\rho/B)(dB/d\rho)$  is independent of  $\rho$ . The F and D magnets have opposite signs of both  $B$  and  $n$ , the same magnitudes, and different lengths, so the orbits curve successively towards and away from the ring center in the F and D magnets. In both magnets the magnitude of the field increases outward from the center of the ring. The closed orbits are a scalloped set of parallel curves, the magnet edges lie on radii from the ring center, and the closed orbits are normal to them.

To make the ring close, the F magnets are made longer than the D magnets, in a ratio of about 3/2, which gives a circumference factor  $R/\rho \sim 5$ .<sup>1</sup> The cells have constant tune values with energy because the transverse focusing equations, when expressed with  $\theta = s/R$  as the independent variable ( $R = \text{circumference}/2\pi$ ), only depend on  $n(\theta)$ , which is independent of energy. Typical cell tunes are  $\mu_x = 5\pi/6, \mu_y = \pi/6$ . For given tunes and field strength, the magnet lengths and radial extent of the closed orbits decrease with increasing values of  $n$ . Arc cell parameters are given in Table 1 and lattice functions plotted in Figure 3.

There are three main advantages of this design: the betatron tunes are independent of energy, the radial width of the orbits can be made very small for a large accelerated energy range, and the variation of orbit lengths is also small. The disadvantages are the large circumference factor and the difficulty of designing superconducting magnets with large  $n$ .

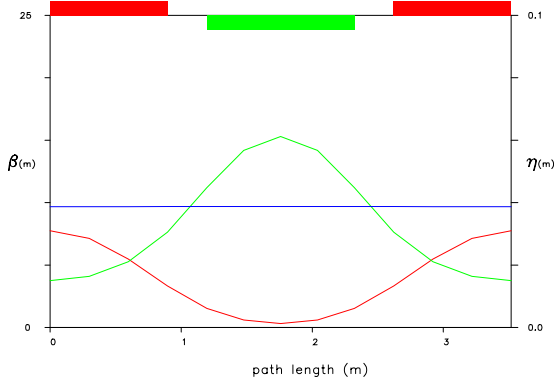


Figure 3: Arc cell with constant field-index magnets

Long straight sections can be included in a scaling radial sector FFAG. One can design matched insertions by using focusing magnets identical to the cell F and D magnets, but with different lengths and spacings. Long straight drift spaces can be placed between triplets, and the dispersion can be reduced to zero in the long drift space by placing pairs of 0-gradient dipoles at each end of the drift. As a result the radial spread of the orbits in the long drifts is reduced from that in the arc cells by a factor of about five. Figure 4 shows a sector of the ring which includes this insertion with a drift straight section.

As an example of a scaling radial sector FFAG accelerator, we consider a ring that might function as the final acceleration stage for a Higgs factory muon collider. It would accelerate muons over an energy factor of about four, say from 16 GeV to 64 GeV.

<sup>1</sup>The magnet lengths and  $|n|$  determine the cell tunes. If the magnet length ratio is too large, the cell is vertically unstable.

Table 1: Arc cell parameters

Lattice: $C = F/2 \ O \ D \ O \ F/2$			
Rigidity at 40 GeV	T-m	$B\rho$	133.4
Magnetic field at 40 GeV	T	$B$	4.86
Gradient at 40 GeV	T/m	$B'$	125
Magnetic field index ( $-B'/B\rho$ )		$n$	707
Magnetic radius	m	$\rho$	27.5
Cell length	m	$L_C$	3.51
F-magnet length	m	$L_F$	1.79
D-magnet length	m	$L_D$	1.13
Drift space length	m	$L_O$	0.8
Cell tune - horizontal		$\mu_x$	0.416
Cell tune - vertical		$\mu_y$	0.084
Horizontal beta maximum	m	$\hat{\beta}_x$	7.8
Vertical beta maximum	m	$\hat{\beta}_y$	15.3
Dispersion (constant in cells)	cm	$D$	3.87

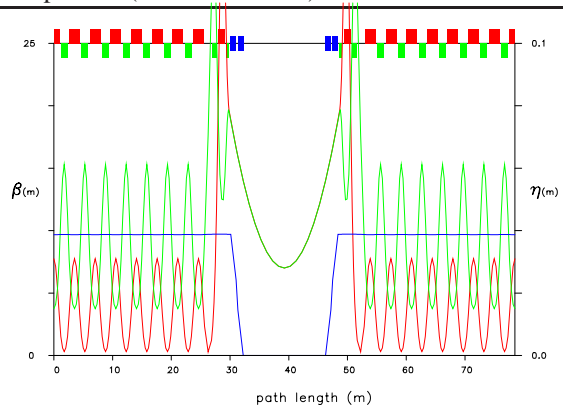


Figure 4: Insertion with 14 m drift space.

The ring lattice is made up of 16 sectors; each sector consists of 14 FODO cells and one insertion containing a 14 meter straight section. A one-period wiggler is installed in every fourth long straight section. The wigglers reduce the variations of circumference with energy. Thus the ring has four superperiods, each containing three sectors with drift straight section insertions and one sector with a wiggler insertion. Four of the drift straight sections are used to inject or extract one of the two muon beams and the other eight drift straight sections contain rf cavities. The total circumference of this ring is 1356 km.

## 5 REFERENCES

- [1] “Muon Collider Status Report”, <http://www.cap.bnl.gov/mumu/status-report.html>
- [2] K Simon, MURA-KRS-6, (MURA-43) (1954); K. Simon, et al, Phys. Rev. **103** p. 1837, (1956).